# Precise determination of charge-dependent pion-nucleon-nucleon coupling constants

R. Navarro Pérez,[1,*] J. E. Amaro,[2,†] and E. Ruiz Arriola[2,‡]

[1]*Nuclear and Chemical Science Division, Lawrence Livermore National Laboratory, Livermore, California 94551, USA*

[2]*Departamento de Física Atómica, Molecular y Nuclear and Instituto Carlos I de Física Teórica y Computacional Universidad de Granada, E-18071 Granada, Spain*

(Received 10 June 2016; revised manuscript received 8 April 2017; published 19 June 2017)

We undertake a covariance error analysis of the pion-nucleon-nucleon coupling constants from the Granada-2013 $np$ and $pp$ database, comprising a total of 6720 scattering data below laboratory energy of 350 MeV. Assuming a unique pion-nucleon coupling constant in the one-pion exchange potential above a boundary radius $r_c = 3$ fm we obtain $f^2 = 0.0763(1)$. The effects of charge symmetry breaking on the ${}^3P_0$, ${}^3P_1$, and ${}^3P_2$ partial waves are analyzed and we find $f_p^2 = 0.0761(4)$, $f_0^2 = 0.0790(9)$, and $f_c^2 = 0.0772(6)$ with a strong anticorrelation between $f_c^2$ and $f_0^2$. We successfully test normality for the residuals of the fit. Potential tails in terms of different boundary radii as well as chiral two-pion-exchange contributions as sources of systematic uncertainty are also investigated.

DOI: 10.1103/PhysRevC.95.064001

## I. INTRODUCTION

The meson exchange picture is a genuine quantum field theoretical feature which implies, in particular, that the strong force between protons and neutrons at long distances is dominated by the exchange of the lightest hadrons compatible with the conservation laws, namely neutral and charged pions. The strong force acting between nucleons at sufficiently large distances or impact parameters $\gtrsim 3$ fm is solely due to one-pion exchange (OPE) and was suggested by Yukawa 80 years ago [1]. The verification of this mechanism provides not only a check of quantum field theory at the hadronic level but also quantitative insight onto the determination of the forces which hold atomic nuclei [2]. While the mass of the pion may be determined directly from analysis of their tracks or electroweak decays, the determination of the coupling constant to nucleons needs further theoretical elaboration. The pion-nucleon-nucleon coupling constant is rigorously defined as the $\pi NN$ vertex function when all three particles are on the mass shell and in principle any process involving the elementary vertices $p \to \pi^0 p$, $n \to \pi^0 n$, $p \to \pi^+ n$, and $n \to \pi^- p$ (or their charge conjugated) is suitable for the determination of the corresponding couplings provided all other relevant effects are accounted for with an acceptable level of precision. In this work, we extract these coupling constants from $NN$ scattering data and look for signals of charge symmetry breaking.

The combinations entering in $NN$ scattering are (we use the conventions of Ref. [3] and when possible, for simplicity, omit the $\pi$ label)

$$f_p^2 = f_{\pi^0 pp} f_{\pi^0 pp}, \tag{1}$$

$$f_0^2 = -f_{\pi^0 nn} f_{\pi^0 pp}, \tag{2}$$

$$2 f_c^2 = f_{\pi^- pn} f_{\pi^+ np}. \tag{3}$$

Usually the charge symmetry breaking is restricted to mass differences by setting $f_p = -f_n = f_c = f_0 = f$. The relevant relationship between the pseudoscalar pion coupling constant, $g_{\pi NN}$, and the pseudovector one, $f_{\pi NN}$, is given by

$$\frac{g^2_{\pi^a NN'}}{4\pi} = \left(\frac{M_N + M_{N'}}{m_{\pi^\pm}}\right)^2 f^2_{\pi^a NN'}, \tag{4}$$

where $N, N' = n, p$ and $\pi^a = \pi^0, \pi^\pm$ (the factor $m_{\pi^\pm}$ is conventional). Thus, we may define $g_0^2$, $g_c^2$, and $g_p^2$. We take $M_p = 938.27231$ MeV as the proton mass, $M_n = 939.56563$ MeV as the neutron mass, and $m_{\pi^\pm} = 139.5675$ MeV as the mass of the charged pion.

There is a long history of determinations of pion-nucleon coupling constants using different approaches. A variety of methods and reactions have been used since the seminal Yukawa paper. A more complete account of the subsequent numerous determinations can be traced from comprehensive overviews [4–6]. Here, we will mainly review determinations based on $NN$ scattering.

In 1940, by looking at deuteron properties [7,8] soon after Yukawa proposed his theory and before the pion was experimentally discovered, Bethe found the common value $f^2 = 0.077$–$0.080$. On a more theoretical ground, based on dispersion relations and the partial conservation of the axial current (PCAC), Goldberger and Treiman deduced a relation between the $\pi NN$ form factor, $G_{\pi NN}(t)$, the nucleon axial coupling constant, $g_A = 1.26$, and the pion weak decay constant, $F_\pi = 93.4(3)$ MeV. The relation $G_{\pi NN}(0) F_\pi = M_N g_A$ [9], shown by Nambu to follow from chiral symmetry [10], is strictly valid at the pion off-shell point, $q^2 = 0$, and numerically it yields $f^2_{\pi NN} = g_A^2 m^2_{\pi^+}/(16\pi F_\pi^2) = 0.072$. Almost simultaneously, Chew proposed [11] to determine it from the occurrence of the pion pole in the renormalized Born approximation, by using an extrapolation method which was implemented soon thereafter for $np$ [12] and $pp$ [13] data. The first direct and quantitative evidence for OPE was found in 1960 by Signell [14] by fitting the neutral pion mass to the

*navarroperez1@llnl.gov
†amaro@ugr.es
‡earriola@ugr.es

 

differential cross section in $p$-$p$ scattering data. The method of partial wave analysis (PWA) was soon afterward used by Macgregor *et al.* [15].

During many years, $\pi N$ scattering determination through fixed-$t$ dispersion relations was advocated as a precision tool, yielding initially $f_c^2 = 0.0790(10)$ [16] and later providing $f_c^2 = 0.0735(15)$ [17] (see also Ref. [18] and references therein). The latest and most accurate $\pi N$ scattering determinations are (i) the one based on the Goldberger-Miyazawa-Oehme (GMO) sum rule [19], $g_c^2/(4\pi) = 14.11(20)$ ($f_c^2 = 0.0783(11)$); (ii) the one using fixed-$t$ dispersion relations, $g_c^2/(4\pi) = 13.76(8)$ [20]; (iii) the most recent one [21,22], based on $\pi N$ scattering lengths, $\pi^- d$ scattering, and the GMO sum rule, yielding $g_c^2/(4\pi) = 13.69(12)(15) = 13.69(19)$. Another source of information has been the $\bar{N}N$ system, as shown by the Nijmegen group [23], providing $f_c^2 = 0.0751(17)$.

The modern era of high-quality $NN$ interactions initiated by the Nijmegen group [24] enabled decrease of $\chi^2/\nu$ from 2 to 1, thanks to the implementation of charge dependence (CD), vacuum polarization, relativistic corrections, and magnetic moments interactions, and a suitable selection criterion for compatible data. Their analysis comprised a total of 4313 $NN$ scattering data. This promoted the determination of the pion-nucleon coupling constant from $np$ and $pp$ scattering to a competitively accurate approach. The main advantage of an $NN$ analysis as compared to the $\pi N$ analysis, which has so far been restricted to charged pions, is that one can determine both neutral and charged-pion coupling constants simultaneously, to search for isospin-breaking effects. The three compatible values, $f_p^2 = 0.0751(6)$, $f_0^2 = 0.0752(8)$, and $f_c^2 = 0.0741(5)$, were determined from $NN$ scattering data [25]. The originally recommended charge-independent value $f^2 = 0.0749(4)$ [25] was revised [26] and confirmed in the 1997 review on the status of the pion-nucleon-nucleon coupling constant [4]; this is the most accurate $NN$ determination to date. There, it was suggested that a charge-independence breaking could be checked with more data and better statistics. The most recent determinations of the Nijmegen group have been given after the inclusion of charge-independent chiral two-pion exchange ($\chi$TPE) potential [27], which depends on three additional chiral constants, $c_1$, $c_3$, $c_4$, which also appear in $\pi N$ scattering. A combined fit of $f_p^2$ and $c_{1,3,4}$ to $pp$ scattering data provides the value $f_p^2 = 0.0756(4)$ [28], and a simultaneous fit to $pp + np$ data of a common $f^2$ and $c_{1,3,4}$ [29] provides linear correlations between $f^2$ and $c_{1,2,3}$.

Most of the analyses determining the pion nucleon coupling constants involve heavy statistical analysis for a large body of experimental data, mostly $\chi^2$ fits, which are subjected to a number of *a posteriori* tests [30]. The verification of these tests buttress a sensible analysis of uncertainties of theoretical models [31]. To the time of their analysis, the Nijmegen group [26,32] checked the statistical quality of $pp$ fit residuals using the moments test, which for increasing orders overweights the tails.

In this paper, we study the possible differences among the pion-nucleon coupling constants by analyzing $np$ and $pp$ scattering data using the $NN$ Granada-2013, $3\sigma$-self consistent database, designed and analyzed recently [33–37]. There, we have selected 6713 out of 8000 published $np$ and $pp$ experimental data for LAB energies below 350 MeV and measured in the period 1950–2013, which satisfactorily verify the tail-sensitive test [38], based on the quantile-quantile plot for the combined $np + pp$ residuals (see also Ref. [39] for an application of these ideas to $\pi\pi$ scattering). As a side remark, we note that the Uppsala controversial measurement [40,41], which gives the value $f^2 = 0.081$ and appears in Weinberg's textbook [42], was disputed by the Nijmegen group [43] and contested [44]. An overview of the situation is provided in Ref. [45]. This measurement has been rejected by our $3\sigma$ self-consistent database [34]. A later remeasurement at IUCF by the partly the same group [46,47], which is compatible with the original Nijmegen PWA, is not rejected by the self-consistent $3\sigma$ criterion.

The paper is organized as follows. In Sec. II, we describe the OPE potential, introduce our notation, and discuss the conditions under which we naturally expect to unveil charge dependence in the pion-nucleon coupling constants. In Sec. III, we review the main aspects of our partial wave analysis and the Granada-2013 database. Our motivation for incorporating charge dependence in the $P$ waves, besides the customary charge dependence on $S$ waves implemented in all modern high quality fits, is presented in Sec. IV along with a discussion of our numerical results based on a covariance analysis. An effort to quantify systematic errors by analyzing the long-range component of the CD-OPE is made in Sec. V. Finally, in Sec. VI conclusions are presented. In Appendix A we show the extended operator basis accommodating $S$-wave and $P$-wave charge dependence.

## II. CHARGE-DEPENDENT ONE-PION EXCHANGE

The charge-dependent, one-pion exchange (CD-OPE) potential incorporates charge symmetry breaking by considering the mass difference of the neutral and charged pions as well as assuming different coupling constants. We use the convention for $\pi NN$ Lagrangians defined in the review of Ref. [3]. The quantum mechanical potential which reproduces in Born approximation the corresponding Feynman diagrams for on-shell static nucleons is given in the $pp$, $nn$, and $np$ channels as

$$V_{\mathrm{OPE},pp}(r) = f_p^2 V_{m_{\pi^0},\mathrm{OPE}}(r), \tag{5}$$

$$V_{\mathrm{OPE},nn}(r) = f_n^2 V_{m_{\pi^0},\mathrm{OPE}}(r), \tag{6}$$

$$V_{\mathrm{OPE},np}(r) = -f_n f_p V_{m_{\pi^0},\mathrm{OPE}}(r) - (-)^T 2 f_c^2 V_{m_{\pi^\pm},\mathrm{OPE}}(r), \tag{7}$$

respectively. Here, $V_{m,\mathrm{OPE}}$ is given by

$$V_{m,\mathrm{OPE}}(r) = \left(\frac{m}{m_{\pi^\pm}}\right)^2 \frac{1}{3} m [Y_m(r)\boldsymbol{\sigma}_1 \cdot \boldsymbol{\sigma}_2 + T_m(r) S_{1,2}]. \tag{8}$$

Here $Y_m$ and $T_m$ are the usual Yukawa functions,

$$Y(r) = \frac{e^{-mr}}{mr} \tag{9}$$

$$T(r) = \frac{e^{-mr}}{mr}\left[1 + \frac{3}{mr} + \frac{3}{(mr)^2}\right], \tag{10}$$

$\sigma_1$ and $\sigma_2$ are the single nucleon Pauli matrices, and $S_{12} = 3\sigma_1 \cdot \hat{\mathbf{r}}\sigma_2 \cdot \hat{\mathbf{r}} - \sigma_1 \cdot \sigma_2$ is the tensor operator. Unfortunately, the CD-OPE potential by itself cannot be directly compared to experimental data, and the only way we know how to determine these pion-nucleon couplings is by carrying out a PWA.

From a purely classical viewpoint, in order to *measure* the nuclear force directly it would just be enough to hold and pull two nucleons apart at distances larger than their elementary size, which is or the order of 2 fm [33]. For such an ideal experiment, the behavior of the system at shorter distances would be largely irrelevant, because nucleons would behave as pointlike particles. This situation would naturally occur if nucleons were truly infinitely heavy. In that case the potential would correspond to the static energy of a system with baryon number $B = 2$ and total charge $Q = 2,1,0$, for $pp$, $pn$, $nn$, respectively.[1] Of course, the quantum mechanical nature of the nucleons prevents such a situation experimentally and we are left with scattering experiments. Good operating conditions are achieved when the maximum relative center of mass (c.m.) momentum, $p_{\max}$, is small enough to avoid complications due to inelastic channels and large enough to contain as many data as possible. This generates a resolution ambiguity of the order of the minimal relative de Broglie wavelength, $\lambda_{\min} = \Delta r \sim 1/p_{\max}$. Since the $NN \to \pi NN$ channel opens up at $p_{\max} \sim \sqrt{m_\pi M_N} \sim 360$ MeV, we have $\Delta r \sim 0.6$ fm. Unfortunately, in the quantum mechanical $NN$ scattering problem the scales are somewhat intertwined, and thus some information on the unknown short-distance components of the potential have to be considered in order to evaluate the scattering amplitude, the cross section, or the polarization asymmetry. The low-energy behavior of the $NN$ interaction is expected to depend strongly on its long-distance properties. Although some coarse-grained information of the unknown contribution is needed, it can be deduced from the experiment with an overall *sufficient* accuracy as to determine the differences between the pion-nucleon couplings. This viewpoint allows us to determine *a priori* the number of independent parameters $N_{\rm Par}$ needed for a successful fit.[2] These ideas where introduced by Aviles [51], and they underlie the recent $NN$ analysis carried out by the present authors, where a large database, comprising about 8000 published experimental data measured in the period 1950–2013, was considered [33,34].

### A. The number of data

There is no symmetry reason why the strong force between protons and between neutrons should be exactly identical; if a difference exists one should be able to see it with a sufficiently large amount of experimental data. These differences are in fact small and hard to pin down because *a priori* the electromagnetic corrections should scale with the fine structure constant $\delta g/g \sim \alpha \sim 1/137$, and the strong (QCD) corrections should scale with the $u - d$ quark mass difference (relative to the $s$-quark mass), which means $\delta g/g \sim (m_u - m_d)/\Lambda_{\rm QCD} \sim (M_p - M_n)/\Lambda_{\rm QCD} \sim 1/100$, for $\Lambda_{\rm QCD} \sim 250$ MeV. This simple estimates suggest that in order to witness isospin violations in the couplings we should determine them with a target accuracy better than 1–2%, which is not too far from the most recent values. On a purely statistical basis, the relative uncertainty due to $N$ independent measurements is $\Delta g/g \sim 1/\sqrt{N}$. If we have some extra parameters $(\lambda_1, \ldots, \lambda_{N_{\rm Par}})$,the condition $\Delta g \sim \delta g \sim 0.01$–$0.02$ would require $N = N_{\rm Dat} - N_{\rm Par} \sim 7000$–$10\,000$ *independent* degrees of freedom. Since $N_{\rm Dat} \gg N_{\rm Par}$ this is comparable to the total amount of existing elastic $np$ and $pp$ scattering data. While these are rough estimates, we stress the independence character of the measurements in order to make these estimates credible; it is not just a question of having more data. From the point of view of $\chi^2$ fits this requires passing satisfactorily normality tests guaranteeing the self-consistency of the fit. In particular, adding many incompatible data would invalidate this analysis.

### B. Naturalness of fitting parameters

While our approach is based on a standard least-squares optimization, which minimizes the distance between the theory and the experiment for many $pp$ and $np$ scattering data, it is important to mention that we do not consider that all fits are eligible and in fact some of them will be rejected. In what follows, we specify these criteria *a priori*.

As a matter of principle, we reject fits which display bound states in channels other than the deuteron (occurring in the $^3S_1$-$^3D_1$ channel only) which will be considered spurious. The appearance of such states in the fitting process is not so unlikely, particularly in the case of peripheral waves. This is usually detected by use of Levinson's theorem, $\delta_l(0) - \delta_l(\infty) = n\pi$, which requires checking phases at energies much larger than the fitting range. An equivalent way to find spurious bound states is by checking the volume integrals (and high moments) for which a large degree of universality has been found [52]. Attractive couplings in the potential permitting a bound state that were too large would consequently generate unnaturally large volume integrals of the potentials.

[1] This is the case in lattice calculations, where static sources are placed at a fixed distance [48,49]. In the quenched approximation, for a pion mass of $m_\pi = 380$ MeV, the value $g^2/(4\pi) = 12.1 \pm 2.7$, which is encouraging [50] but still a crude estimate.

[2] In Ref. [33] it was found that, for $r_c = 3$ fm, the number of needed parameters is $N_{\rm Par} \sim 60$. The argument is based on the idea that, if we adopt the CD-OPE potential above $r_c$, we can estimate the number of independent potential values $V(r_n)$ below $r_c$ in any partial wave channel, with $r_n = n\Delta r$. Since the maximum angular momentum in the partial wave expansion is $l_{\max} \sim p_{\max} r_c$ and there are four independent waves for each $l$, we would have $N_{\rm Par} \sim 4 l_{\max}(r_c/\Delta r)$. Excluding the points $r_n$ below the centrifugal barrier, the number becomes $N_{\rm Par} \sim 2(p_{\max} r_c)^2$.

In the case of the pion-nucleon coupling constant, we expect some theoretical constraints to be fulfilled. The renowned Goldberger-Treiman relation was deduced as a consequence of exact PCAC, and yields the value (in the isospin limit)

$$G_{\pi NN}(0) = M_N g_A / F_\pi . \tag{11}$$

The physical coupling constant corresponds to $g_{\pi NN} \equiv G_{\pi NN}(m_\pi^2) > G_{\pi NN}(0)$. It is expected to be *larger* than value appearing in GT relation. This suggests

$$g_{\pi NN} > M_N g_A / F_\pi \tag{12}$$

and hence, for the PDG values $F_{\pi^+}^{\rm PDG} = 92.21(14)$MeV and $g_A = 1.2723(23)$,

$$f_{\pi NN}^2 > f_{\pi NN,{\rm GT}}^2 \equiv \frac{1}{16\pi}\left(\frac{g_A m_{\pi^+}}{F_\pi}\right)^2 = 0.07324(4). \tag{13}$$

The uncertainty is about 5%. More generally, a GT discrepancy is defined (see, e.g., Ref. [53] for a review) as

$$\Delta_{\rm GT} = 1 - \frac{M_N g_A}{g_{\pi NN} F_\pi}. \tag{14}$$

The value of this number has been changing but typical values nowadays are at the few percent level, $\Delta_{\rm GT} \sim 0.01$–$0.03$. In the limit of zero quark masses, chiral symmetry becomes exact, and hence $\Delta_{\rm GT} = \mathcal{O}(m_\pi^2/F_\pi^2)$.

The fact that $(m_u - m_d)/(m_u + m_d) \sim 1/3$ suggests that, if we obtain a GT discrepancy different from zero, about three more times precision would be needed to pin down isospin breaking. According to our $1/\sqrt{N_{\rm Dat}}$ estimate above, this can be accomplished by increasing the number of independent data by a factor of 10. At the level of isospin breaking, some estimates have also been made [54,55].

In the case of $\chi$TPE exchange, which will also be considered below, the chiral constants $c_{1,3,4}$ are saturated by meson exchange [56]. Actually, $c_1$ is saturated by scalar exchange. The saturation value is $c_1^S = -g_S c_m / m_S^2$. Taking $M_N = g_S F_\pi$ and $c_m = F_\pi/2$, $m_S = m_V = F_\pi\sqrt{24\pi/N_c}$ [57] and $M_N = N_c m_\rho/2$, we get $c_1^S \sim -N_c/(4\sqrt{2}m_\rho) \sim -0.7$ GeV$^{-1}$. In the case of the constants $c_3$ and $c_4$, they are saturated by $\Delta$ resonance; taking $\Delta = M_\Delta - M_N$, the saturation values are $c_2^\Delta = -c_3^\Delta = 2c_4^\Delta = g_A^2/(2\Delta) \sim 2.97\,{\rm GeV}^{-1}$. Of course, these are not very accurate values, but indicate the order of magnitude one should expect.

## III. THE GRANADA-2013 ANALYSIS

In a series of works, we have upgraded the $NN$ database to include a total of 6720 $np$ and $pp$ published experimental data by using a coarse grained representation of the interaction, and applying stringent statistical tests on the residuals of the $\chi^2$ fits after implementing a $3\sigma$ self-consistent selection process [35]. The resulting Granada-2013 is at present the largest $NN$ database, which can be described by a CD-OPE contribution. There are about 60% more data than the 4313 data used in the latest Nijmegen upgrade [4]. This suggests that we can improve on the errors for the pion-nucleon couplings, as discussed in the previous section.

We have discussed in detail the many issues in carrying out the data selection, the fit, and the corresponding joint $np + pp$ partial wave analysis. We review here the main aspects as a guideline and refer to those works for further details.

We separate the potential into two well-defined regions depending on a chosen cutoff radius, $r_c$, fixed in such a way that for $r > r_c$ the CD-OPE is the only strong contribution. In addition, for $r > r_c$ we also include electromagnetic (Coulomb, vacuum polarization, magnetic moments) [34] and relativistic corrections, which we simply add to the strong potential:

$$V(\mathbf{r}) = V_{\rm OPE}(\mathbf{r}) + V_{\rm EM}(\mathbf{r}), \quad r > r_c. \tag{15}$$

Below the cutoff radius, $r < r_c$, we regard the $NN$ force as unknown, and we use $\delta$ shells located at equidistant points separated by $\Delta r = 0.6$ fm, corresponding to the shortest de Broglie wavelength at pion production threshold. The fitting parameters are the real coefficients $(\lambda_i)_{ll'}^{JS}$ for each partial wave:

$$V_{l,l'}^{JS}(r) = \frac{1}{2\mu}\sum_{i=1}^{N}(\lambda_i)_{ll'}^{JS}\delta(r - r_i), \quad r \leqslant r_c, \tag{16}$$

where $\mu$ is the $NN$ reduced mass. Alternatively, the potential can be expanded in an operator basis extending the AV18 potentials in coordinate space; see Appendix A. The transformation between partial wave and operator basis was given in Ref. [34].

It turns out that $r_c = 3$ fm provides statistically satisfactory fits to the selected $3\sigma$ self-consistent Granada-2013 database. While it would be interesting to separate explicitly the known from the unknown pieces of the interaction below the cutoff radius $r_c$, this is actually a complication in the fitting procedure and will not change the values of the most likely pion-nucleon coupling constants. Another advantage of taking $r_c = 3$ fm is that in our analysis there is no need of form factors of any kind, and thus we are relieved from disentangling finite-size effects, quark exchange, and the intrinsic resolution $\Delta r$ inherent to any finite-energy PWA.[3]

The possible $A_y$ problem for $np$ scattering, raised by the data of Ref. [59], suggested a sizable isospin breaking of coupling constants. The problem was reanalyzed theoretically in Ref. [60] and motivated the reanalysis of the data [61] and the disentanglement between systematic and statistical errors. Actually, in Ref. [60] it was found that these data might be explained in an isolated fashion when isospin was broken. Thus, we allow this isospin breaking to foresee the possibility of recovering the data.

## IV. STATISTICAL ANALYSIS

In our previous analysis, we took a fixed common value for the pion-nucleon coupling constant suggested by the Nijmegen group. When we relax this assumption and also fit the pion-nucleon coupling constant as another parameter in the potential, we obtain $f^2 = 0.0763(1)$, which is $3\sigma$ compatible with the Nijmegen recommendation [25], $f^2 = 0.0749(4)$, and more accurate.

[3] An explanation of the apparent charge dependence of the pion-nucleon coupling was attributed to the strong form factor [58].

### A. Charge symmetry breaking on S and P waves

An old problem in $NN$ scattering fitting is if it is possible to predict the neutron-neutron potential fron $np$ and $pp$ data. A necessary condition would be that the unknown piece of the short-distance interaction for $np$ and $pp$ coincide in the isovector channels. Once we vary the coupling constants $f_p^2$, $f_0^2$, and $f_c^2$ from their common value $f^2$, we have first searched for a fit *without* CD in the $\lambda's$ (i.e., assuming that they are equal for $np$ and $pp$). We get $\chi^2/\nu = 1.2$ for CD-OPE above $r_c = 3$ fm. On the other hand, $\chi^2/\nu = 9$ for CD-OPE + $\chi$TPE above $r_c = 1.8$ fm. Therefore, and in harmony with all high-quality previous attempts, we cannot deduce $nn$ scattering below $r_c = 3$ fm.

Following the common practice of other analyses [24,62,63], we have previously allowed different $pp$ and $np$ parameters only on the $^1S_0$ partial wave [33,34,64,65] and found that this symmetry breaking is indeed necessary to obtain an accurate description of the $pp$ and $np$ scattering data. The large collection of about 8000 available data also makes it possible to test charge symmetry breaking on the parametrization of higher partial waves, e.g., $^3P_0$, $^3P_1$, and $^3P_2$.

To carry out such a test, we have considered different $np$ and $pp$ parameters on those partial waves and performed a full PWA and selection process as described in Refs. [34,65], by fitting the $\delta$-shell potential parameters to the complete database and then applying the $3\sigma$ rejection criterion iteratively until a self-consistent database is obtained. The consistent database obtained in this case has 3006 $pp$ data and 3735 $np$ data, including normalizations, and the value for the $\chi^2$ per number of data is $\chi^2/N_{\rm data} = 1.02$. When compared with our previous consistent database [34], this symmetry breaking can only describe 21 additional data out of more than 1000 rejected data. Figure 1 compares the low-angular-momentum phase shifts of the PWA in Ref. [34] (blue bands) with this new analysis (red bands). The $pp$ phase shifts show no significant difference, while the $np$ ones are statistically different and the differences are even greater for higher-angular-momentum partial waves. Tabulated values for the lower phase shifts for selected LAB energies are provided in Appendix B.

Usually the charge symmetry breaking is restricted to mass differences by setting $f_p = -f_n = f_c = f$. The value $f^2 = 0.075$ recommended by the Nijmegen group [25] has been used in most of the potentials since the seminal 1993 partial wave analysis [24]. Here we test this charge independence with the large body of data available today, by using $f_p$, $f_0$, and $f_c$ as extra fitting parameters along with the previous 46 $\delta$-shell parameters. We show our results in Table I, depending on different strategies regarding isospin breaking: $S$ waves, $S$ and $P$ waves, and in the coupling constants. The working group summary of 1999 provides a recent compilation of coupling constants in a chronological display [5]. The most recent determination [21,22], based on $\pi N$ scattering lengths and $\pi^- d$ scattering, and in the GMO sum rule, yields $g_c^2/(4\pi) = 13.69(12)(15) = 13.69(20)$. From our full covariance matrix analysis, we get $g_p^2/(4\pi) = 13.774(75)$, $g_0^2/(4\pi) = 14.30(16)$, and $g_c^2/(4\pi) = 13.984(82)$. The last value is $2\sigma$ compatible with these determinations, but slightly more accurate.

The fitting $\delta$-shell parameters obtained in our different strategies, regarding charge independence breaking in just $S$ waves and charge independence breaking in $S$ and $P$ waves, can be seen in Tables II and III respectively. We use the resulting parameters along with their covariance matrix to calculate $f_p^2$, $f_0^2$, and $f_c^2$, and propagate the corresponding statistical uncertainties and test charge dependence. Figure 2 shows the $1\sigma$ correlation ellipses along with the scatter diagram resulting from drawing 1000 random variations following the multivariate normal distribution dictated by the covariance matrix. The fit without charge dependence on the $P$ waves is indicated by the blue dots and yellow line while the fit with charge dependence on the $P$ waves corresponds to the red diamonds and green line. Charge independence, $f_p^2 = f_0^2 = f_c^2$, is marked by the diagonal black line. Several aspects should be noted from Fig. 2. First, while the values on Table I seem to suggest that the determinations with and without charge charge-dependent $P$ waves for $f_0^2$ and $f_c^2$ are 1 and $2\sigma$ compatible respectively, in fact the strong anticorrelation between the two coupling constants makes the determinations completely incompatible. The determination with charge dependence on the $S$ waves only is compatible with the $f_p^2 = f_0^2 = f_c^2 = 0.0763(1)$ fit at the $2\sigma$ level; this is in accordance with the slight decrease in $\chi^2$ in spite of the fact that two extra parameters are fitted. Finally, the fit with charge-dependent $P$ waves is incompatible with $f_p^2 = f_0^2 = f_c^2$, once again due to the strong anticorrelation between $f_0^2$ and $f_c^2$.

### B. Normality tests

The standard assumption underlying a conventional $\chi^2$ fit is that the sum of $\nu$-independent squared Gaussian variables belonging to the normal distribution $N(0,1)$ follows a $\chi^2$ distribution with $\nu$ degrees of freedom [30]. One can actually check *a posteriori* if the outcoming residuals do indeed fulfill the initial assumption with a given confidence level. The self-consistency of the fit is an important test, since it validates the current statistical analysis and provides some confidence on the increase in accuracy that we observed as compared to previous works. For a number of data much larger than the number of fitting parameters, $N_{\rm Dat} \gg N_{\rm Par}$, the conventional $\chi^2$ test requires

$$N_\sigma = \frac{\left|\chi^2_{\rm min}/\nu - 1\right|}{\sqrt{2/\nu}} \tag{17}$$

with $\nu = N_{\rm Dat} - N_{\rm Par}$ for a $N_\sigma$ standard deviation confidence level. The tail-sensitive normality test is more demanding and the three fits presented on this section are summarized in Fig. 3 as rotated quantile-quantile plots. The tail-sensitive test compares the empirical quantiles of the residuals with the expected ones from an equally sized sample from the standard normal distribution. The red bands represent the 95% confidence intervals of the normality test. For more details of the tail-sensitive test, see Ref. [36].

### C. Separate contributions to the fit

In line with previous studies, it is interesting to decompose the contributions to the total $\chi^2$ both in terms of the fitted

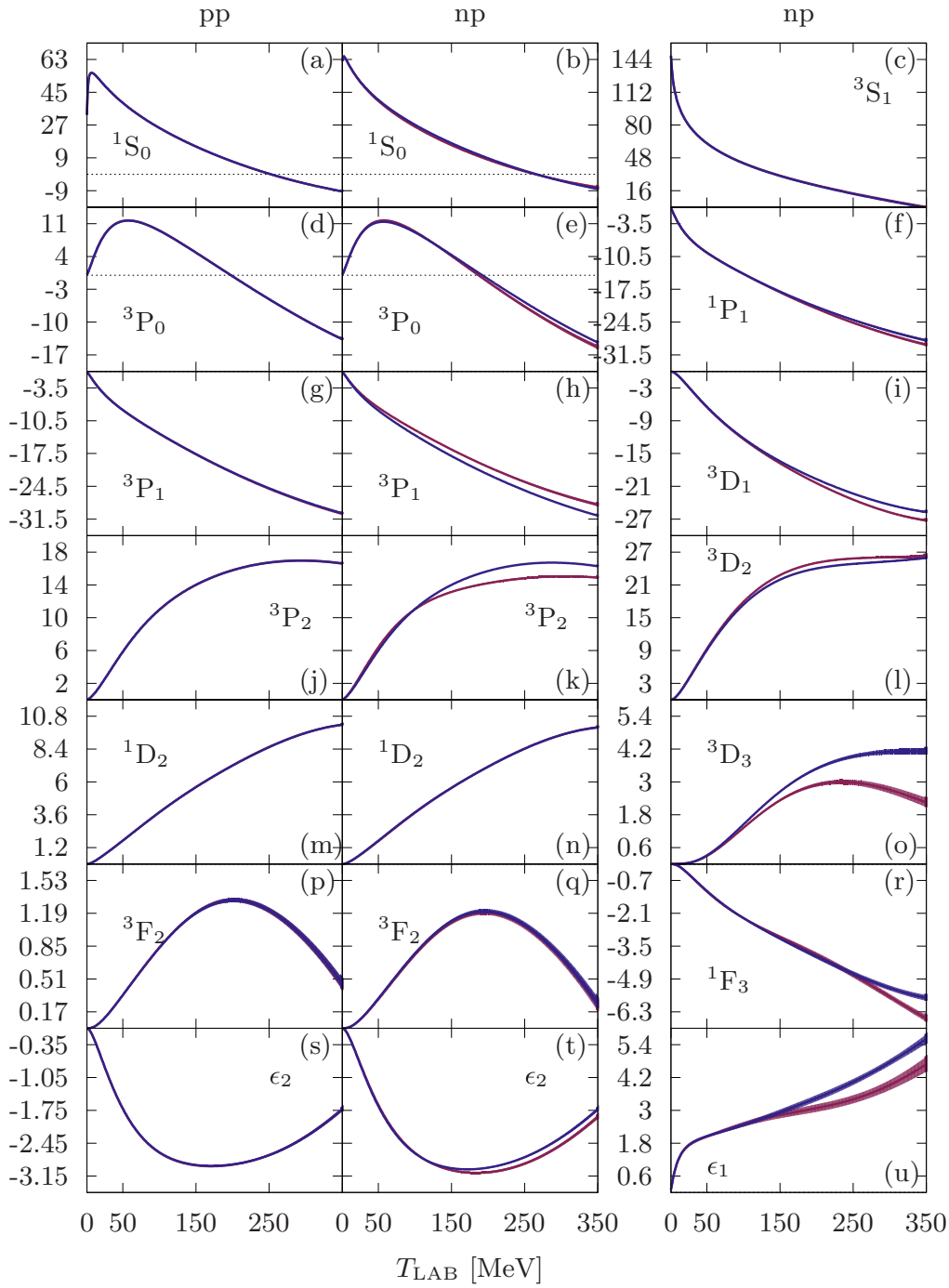


FIG. 1. Phase shifts obtained from a partial-waves analysis to *pp* and *np* data and statistical uncertainties. Blue band from Ref. [34] and red band from a fit with charge symmetry breaking on the $^3P_0$, $^3P_1$, and $^3P_2$ partial waves.

TABLE I. The pion-nucleon coupling constants $f_p^2$, $f_0^2$, and $f_c^2$ determined from different fits to the Granada-2013 database and their characteristics. We indicate the partial waves where charge dependence is allowed.

| $f_p^2$ | $f_0^2$ | $f_c^2$ | CD waves | $\chi^2_{pp}$ | $\chi^2_{np}$ | $\chi^2$ | $N_{\rm Dat}$ | $N_{\rm Par}$ | $\chi^2/\nu$ |
|---|---|---|---|---|---|---|---|---|---|
| 0.075 | | | $^1S_0$ | 2997.29 | 3957.57 | 6954.86 | 6720 | 46 | 1.042 |
| 0.0763(1) | | | $^1S_0$ | 2995.20 | 3952.85 | 6947.05 | 6720 | 47 | 1.041 |
| 0.0764(4) | 0.0779(8) | 0.0758(4) | $^1S_0$ | 2994.41 | 3950.42 | 6944.83 | 6720 | 49 | 1.041 |
| 0.0761(4) | 0.0790(9) | 0.0772(5) | $^1S_0$, $P$ | 2979.37 | 3876.13 | 6855.50 | 6741 | 55 | 1.025 |

TABLE II. Fitting $\delta$-shell parameters $(\lambda_n)^{JS}_{l,l'}$ (in fm$^{-1}$) with their errors for all states in the $JS$ channel for a fit with isospin symmetry breaking on the $^1S_0$ partial wave parameters only and the pion-nucleon coupling constants $f_0^2$, $f_p^2$, and $f_c^2$ as fitting parameters We take $N = 5$ equidistant points with $\Delta r = 0.6$ fm. An empty cell indicates that the corresponding fitting $(\lambda_n)^{JS}_{l,l'} = 0$. The lowest part of the table shows the resulting OPE coupling constants with errors

| Wave | $\lambda_1$ | $\lambda_2$ | $\lambda_3$ | $\lambda_4$ | $\lambda_5$ |
|---|---|---|---|---|---|
| $^1S_{0np}$ | 1.16(6) | −0.77(2) | −0.15(1) | | −0.024(1) |
| $^1S_{0pp}$ | 1.31(2) | −0.716(5) | −0.192(2) | | −0.0205(4) |
| $^3P_0$ | | 0.94(2) | −0.319(7) | −0.062(3) | −0.023(1) |
| $^1P_1$ | | 1.20(2) | | 0.075(2) | |
| $^3P_1$ | | 1.354(5) | | 0.0570(5) | |
| $^3S_1$ | 1.79(7) | −0.47(1) | | −0.072(2) | |
| $\varepsilon_1$ | | −1.65(2) | −0.33(2) | −0.233(7) | −0.018(3) |
| $^3D_1$ | | | 0.40(1) | 0.070(9) | 0.021(3) |
| $^1D_2$ | | −0.20(1) | −0.206(3) | | −0.0187(3) |
| $^3D_2$ | | −1.01(3) | −0.17(2) | −0.237(6) | −0.016(2) |
| $^3P_2$ | | −0.482(1) | | −0.0289(7) | −0.0037(4) |
| $\varepsilon_2$ | | 0.32(2) | 0.190(4) | 0.050(2) | 0.0127(6) |
| $^3F_2$ | | 3.50(6) | −0.229(5) | | −0.0140(5) |
| $^1F_3$ | | | 0.12(2) | 0.089(8) | |
| $^3D_3$ | | 0.54(2) | | | |
| $f_p^2$ | | $f_0^2$ | | $f_c^2$ | |
| 0.0764(4) | | 0.0779(8) | | 0.0758(4) | |

TABLE III. Same as Table II for a fit with isopsin symmetry breaking on the $^1S_0$, $^3P_0$, $^3P_1$, and $^3P_2$ partial waves parameters. Asterisks (*) indicate that the $np$ parameter is fixed to be the same as the $pp$ parameter.

| Wave | $\lambda_1$ | $\lambda_2$ | $\lambda_3$ | $\lambda_4$ | $\lambda_5$ |
|---|---|---|---|---|---|
| $^1S_{0np}$ | 1.07(4) | −0.708(7) | −0.192(2)* | | −0.0205(3)* |
| $^1S_{0pp}$ | 1.31(2) | −0.717(5) | −0.192(2) | | −0.0205(3) |
| $^3P_{0np}$ | | 0.95(3) | −0.31(1) | −0.079(4) | −0.019(1) |
| $^3P_{0pp}$ | | 0.94(2) | −0.319(7) | −0.063(3) | −0.022(1) |
| $^1P_1$ | | 1.27(2) | | 0.068(2) | |
| $^3P_{1np}$ | | 1.21(2) | | 0.051(1) | |
| $^3P_{1pp}$ | | 1.364(5) | | 0.0570(6) | |
| $^3S_1$ | 1.54(7) | −0.39(1) | | −0.071(2) | |
| $\varepsilon_1$ | | −1.69(2) | −0.36(2) | −0.233(8) | −0.016(3) |
| $^3D_1$ | | | 0.44(2) | 0.07(1) | 0.014(3) |
| $^1D_2$ | | −0.19(1) | −0.207(3) | | −0.0186(3) |
| $^3D_2$ | | −0.97(5) | −0.21(2) | −0.234(8) | −0.016(2) |
| $^3P_{2np}$ | | −0.445(4) | | −0.043(2) | −0.0024(7) |
| $^3P_{2pp}$ | | −0.483(1) | | −0.0282(7) | −0.0040(4) |
| $\varepsilon_2$ | | 0.30(2) | 0.191(4) | 0.051(2) | 0.0123(6) |
| $^3F_2$ | | 3.41(7) | −0.222(5) | | −0.0142(6) |
| $^1F_3$ | | | 0.23(2) | 0.061(6) | |
| $^3D_3$ | | 0.76(3) | | | |
| $f_p^2$ | | $f_0^2$ | | $f_c^2$ | |
| 0.0761(4) | | 0.0790(9) | | 0.0772(5) | |

observables as well as in different energy bins. The separation is carried out explicitly in Tables IV and V for $pp$ and $np$ scattering observables respectively. As we can see, the size of the contributions $\chi^2/N$ are at similar levels for most observables. Note that observables with a considerable larger or smaller $\chi^2/N$ are also observables with a small number of data, and therefore larger statistical fluctuations are expected.

Likewise, we can also break up the contributions in order to see the significance of different energy intervals; see Table VI. We find that, in agreement with the Nijmegen analysis (see Refs. [66,67] for comparisons with previous potentials), there is a relatively large degree of uniformity in describing data at different energy bins.

## V. ANALYSIS OF SYSTEMATIC ERRORS

In this section, we seek to identify some sources of systematic errors. Besides the success of our fits on purely statistical grounds, it is helpful at this point to analyze why we have chosen our potential representation and the possible systematic uncertainties related to it.

### A. Anatomy of the potential

The present approach uses a coarse-grained interaction in the unknown region, below a cutoff radius $r_c = 3$ fm. The choice of $r_c = 3$ fm, however, is not arbitrary nor blind and in fact it has been guided by a detailed analysis of existing $NN$ forces. We have checked that high-quality potentials used in the past are local at large distances and do implement CD-OPE as the main contribution above 3 fm of strong origin. We note that a plain extrapolation of the CD-OPE potential down to the origin presents a short-distance $1/r^3$ singularity and a certain regularization is needed, which becomes innocuous at $r > r_c = 3$ fm. We have also analyzed quark models from a cluster viewpoint, where there appears to be a form factor naturally regulating electromagnetic Coulomb, OPE, and TPE interactions only below $r_c = 1.8$–$2$ fm [33,70], so that we can assume that nucleons interact, exchanging one or two pions as pointlike particles for distances larger than $r_c > 1.8$ fm. Actually, this assumption can be validated since lowering down to $r_c = 1.2$ fm results in large $\chi^2/\nu$ values (see, e.g., Refs. [71,72] for a discussion within chiral perturbation theory).

One good motivation to analyze the $NN$ interaction is the possible application to nuclear structure calculations. However, the nuclear many-body problem is difficult enough to make specific techniques not suitable for all representations of the interaction; the form of the potential matters. Thus, quite often, potential fitting data are designed to be suitable for a specific technique. This choice introduces a bias which acts as a source of systematic errors. In our previous work [73], we have addressed the systematic uncertainties arising from using several tails and short-distance forms of the potential. The purpose there was to devise a smooth and nonsingular potential in the inner region, friendly for nuclear structure applications, since it turns out that the $\delta$ shells produce a long high-momentum tail which hinders the nuclear structure calculations. This includes some bias because, similarly to other local potentials, smoothness is not a requirement of any physical significance. Thus, these systematic uncertainties stem from a prejudice on insisting in a particular form of the

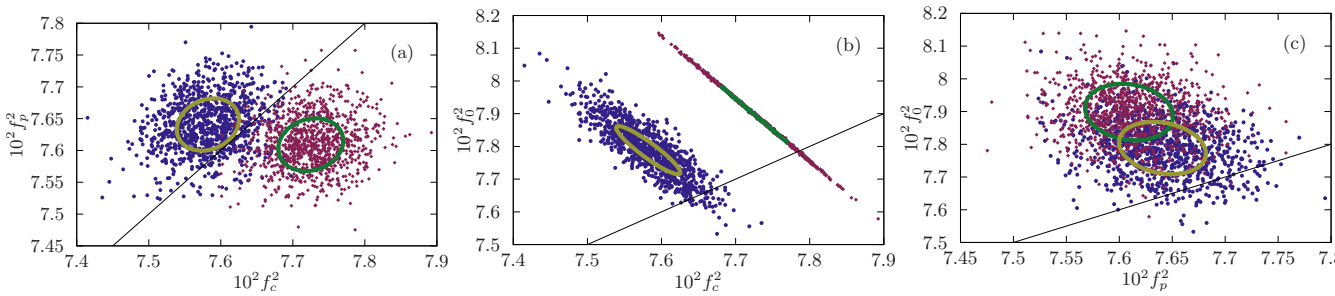


FIG. 2. Correlation ellipses and scatter diagrams for the coupling constants $f_c^2$, $f_p^2$, and $f_0^2$ appearing in the OPE potential from a PWA with (yellow line and blue dots) and without (green line and red diamonds) charge independence on the $P$ waves and a $3\sigma$ consistent database. The black diagonal line indicates $f_c^2 = f_p^2 = f_0^2$.

potential based on its possible application in theoretical nuclear physics and are relevant within that context.

### B. Sampling scale

The motivation for the coarse-grained short-distance potential has been given many times. The sampling scale $\Delta r \sim 1/p_{\max}$ might be varied from its Nyquist optimal sampling value. For a finite-range potential that means sampling with more points since $r_c = n\Delta r$. We generally find that increasing the number of $\delta$ shells results in overfitting; i.e., it does not improve the quality of the fit but it does increase the correlations among the fitting $\lambda_i$'s parameters, exhibiting a parameter redundancy. Correlation plots for this optimal sampling situation have been presented in Ref. [35] for the short-distance parameters and in Ref. [36] for the corresponding counterterms. As it has been discussed in a recent work [74], the Nyquist sampling works up to LAB energies as high as 3 GeV.

### C. Boundary radius

In the previous section, we have assumed a fixed cutoff radius $r_c = 3$ fm, above which a CD-OPE potential is assumed. Here, we analyze the robustness of our determination by modifying the cutoff radius, looking for the cases $r_c =$ 1.8,2.4,3.0, and 3.6 fm. Although the reasons for choosing $r_c = 3$ fm have been explained in Subsec. V A, the variation of the cutoff radius allows us to explore the dependence of the statistical analysis on the particular form of the potential. While this type of cutoff variation in coordinate space is not entirely equivalent to a cutoff variation in momentum space, it can provide insight into cutoff dependence in the latter. Our results are summarized in Table VII. For each value of $r_c$, three PWA are performed. In the first one, the coupling constant $f$ is fixed and not fitted. In the second PWA, a common coupling constant $f$ is fitted as a parameter. In the third one, the three constants $f_p, f_0$, and $f_c$ are fitted as distinct parameters.

Several interesting features are worth mentioning. When the short-distance cutoff is shifted toward smaller values, the $\chi^2/\nu$ increases several times more than the standard statistical tolerance $1 \pm \sqrt{2/\nu}$. Larger $\chi^2/\nu$ values generate smaller uncertainties. This was expected, and it is just a consequence of the larger penalty to change parameters in a worse fit.

As we see, the best global $\chi^2$ (and nearly equal) values are obtained for $r_c = 3$ fm and $r_c = 3.6$ fm. However, we observe that, in going from $r_c = 3.0$ to $r_c = 3.6$, the value of $\chi^2_{pp}$ increases by 40 (with 13 more parameters), whereas the $\chi^2_{np}$ result decreases by 50. Increasing the cutoff means replacing the CD-OPE dependence between 3 and 3.6 by unknown interactions so that many more partial waves will be charge dependent, increasing the number of parameters. At this point, the number of CD parameters becomes rather

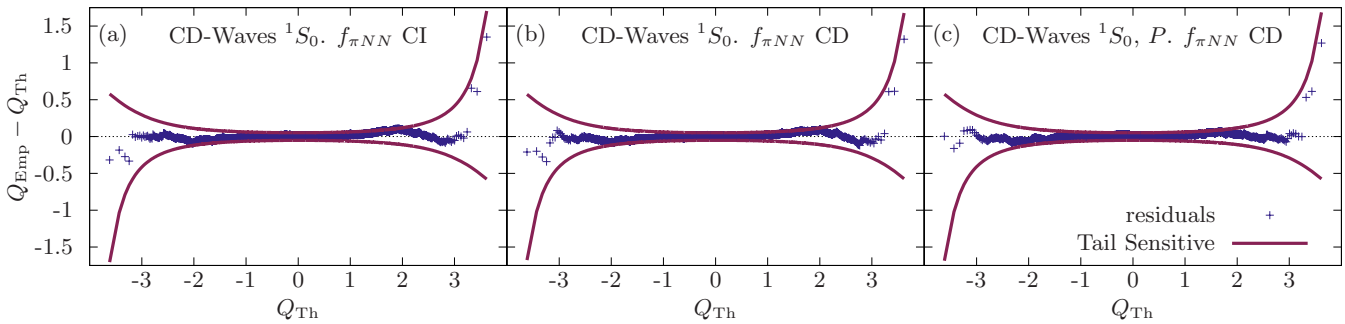


FIG. 3. Rotated quantile-quantile plots for the fits introduced in this work. All points should be inside the confidence band to state that residuals of the fit follow a normal distribution $N(0,1)$, in which case the fit is self-consistent *a posteriori*. Left panel, assuming a charge-independent pion-nucleon constant used as a fitting parameter and charge symmetry breaking only on the $^1S_0$ partial wave parameters. Central panel, assuming three different charge-dependent pion-nucleon constants used as a fitting parameters and charge symmetry breaking only on the $^1S_0$ partial wave parameters. Right panel, assuming three different charge-dependent pion-nucleon constants used as a fitting parameters and charge symmetry breaking on the $^1S_0$ and $P$ partial wave parameters

TABLE IV. Contributions to the total $\chi^2$ for different $pp$ observables. We use the notation of Refs. [68,69].

| Observable | Code | $N_{pp}$ | $\chi^2_{pp}$ | $\chi^2_{pp}/N_{pp}$ |
|---|---|---|---|---|
| $d\sigma/d\Omega$ | DSG | 935 | 903.5 | 0.97 |
| $A_{yy}$ | AYY | 312 | 339.0 | 1.09 |
| $D$ | D | 104 | 135.1 | 1.30 |
| $P$ | P | 807 | 832.4 | 1.03 |
| $A_{zz}$ | AZZ | 51 | 47.4 | 0.93 |
| $R$ | R | 110 | 112.8 | 1.03 |
| $A$ | A | 79 | 70.5 | 0.89 |
| $A_{xx}$ | AXX | 271 | 250.7 | 0.92 |
| $C_{kp}$ | CKP | 2 | 3.1 | 1.57 |
| $R'$ | RP | 29 | 11.9 | 0.41 |
| $M_{s'0sn}$ | MSSN | 18 | 13.1 | 0.73 |
| $N_{s'0kn}$ | MSKN | 18 | 8.5 | 0.47 |
| $A_{zx}$ | AZX | 264 | 250.6 | 0.95 |
| $A'$ | AP | 6 | 0.8 | 0.14 |

large. Furthermore, for $r_c = 3.6$, the values obtained for the $pn$ coupling constants are excluded as unnatural by the Goldberger-Treiman relation shown in Eq. (13).

### D. Adding chiral potential tails

The Nijmegen group estimated systematic errors by including different potential tails, particularly with heavy boson exchange (HBE). More recently, the inclusion of charge-independent chiral two-pion exchange ($\chi$TPE) potential [27], depending on three chiral constants, $c_1$, $c_3$, $c_4$, which also appear in $\pi N$ scattering, allowed them to perform a combined fit of $f_p^2$ and $c_{1,3,4}$ to $pp$ scattering data, obtaining the value $f_p^2 = 0.0756(4)$ [28], and a simultaneous fit to $pp + np$ data of a common $f^2$ and $c_{1,3,4}$ [29].

TABLE V. Contributions to the total $\chi^2$ for different $np$ observables. We use the notation of Refs. [68,69].

| Observable | Code | $N_{np}$ | $\chi^2_{np}$ | $\chi^2_{np}/N_{np}$ |
|---|---|---|---|---|
| $d\sigma/d\Omega$ | DSG | 1712 | 1803.4 | 1.05 |
| $D_t$ | DT | 88 | 83.7 | 0.95 |
| $A_{yy}$ | AYY | 119 | 96.0 | 0.81 |
| $D$ | D | 29 | 37.1 | 1.28 |
| $P$ | P | 977 | 941.7 | 0.96 |
| $A_{zz}$ | AZZ | 89 | 108.1 | 1.21 |
| $R$ | R | 5 | 4.5 | 0.91 |
| $R_t$ | RT | 76 | 72.2 | 0.95 |
| $R'_t$ | RPT | 4 | 1.4 | 0.35 |
| $A_t$ | AT | 75 | 77.0 | 1.03 |
| $D_{0s''0k}$ | D0SK | 29 | 44.0 | 1.52 |
| $N_{0s''kn}$ | NSKN | 29 | 25.5 | 0.88 |
| $N_{0s''sn}$ | NSSN | 30 | 20.3 | 0.68 |
| $N_{0nkk}$ | NNKK | 18 | 13.5 | 0.75 |
| $A$ | A | 6 | 2.9 | 0.49 |
| $\sigma$ | SGT | 411 | 500.2 | 1.22 |
| $\Delta\sigma_T$ | SGTT | 20 | 26.3 | 1.31 |
| $\Delta\sigma_L$ | SGTL | 16 | 18.4 | 1.15 |

In Table VIII, we show several fits of the pion-nucleon coupling constant $f^2$ after including the $\chi$TPE with different cut radius $r_c$ on the analysis. In our previous work [64,71,75], we determined the value of the chiral constants $c_1$, $c_3$, and $c_4$ from $NN$ data while maintaining $f$ fixed. A benefit of implementing $\chi$TPE is that we can generally lower the boundary radius $r_c$ down to the elementary radius, $r_e = 1.8$ fm, with a smaller number of parameters. The outgoing values of the chiral constants should be compared with the recent reanalysis in $\pi N$ scattering using a great deal of theoretical constraints [76]. As with the case of including only CD-OPE on the potential tail, the Goldberger-Treiman relation excludes the fits with $r_c = 3.6$ fm. The unnaturally large values for the chiral constants also call into question the analysis with $r_c = 3.0$ fm and $r_c = 2.4$. Finally, lowering the boundary all the way to $r_c = 1.2$ fm no longer gives a satisfactory description of the data, as indicated by the large value of $\chi^2/\nu$, which is several standard deviations away from the most likely value.

### E. Sensitivity to particular data

The selected database provides $3\sigma$ consistent values for the $\chi^2$ distribution. An important issue concerns the dependence of our results on the chosen data. We do not expect all data to contribute equally to the determination of the coupling constants. In the past, selected data or dedicated experiments have been used to extract the coupling constant. Our analysis rests on a global fit, but it is still interesting to identify the most significant data in the fit of the coupling constant $f^2$.

From a statistical point of view, this can be done by looking at the simplest case, the variations $\Delta\chi^2$ due only to variations on $f$, and by identifying the largest contributions.

The Hessian involving any two fitting parameters $p_i$ and $p_j$ is in general given by

$$\frac{1}{2}\frac{\partial^2\chi^2}{\partial p_i \partial p_j} \approx \sum_{n=1}^{N_{\rm Dat}} \frac{1}{\sigma_n^2}\frac{\partial O_n}{\partial p_i}\frac{\partial O_n}{\partial p_j}, \tag{18}$$

where the standard approximation of neglecting second derivatives has been made. Here $O_n$ is the $n$th observable in the fit and $\sigma_n$ is the experimental error. We can look at this sum for one fitting parameter such as the coupling $f$ *after* ordering the contributions to the Hessian according to their size, i.e., $n \to \pi(n)$,

$$\frac{1}{\sigma_{\pi(n)}}\left|\frac{\partial O_{\pi(n)}}{\partial f}\right| > \frac{1}{\sigma_{\pi(n-1)}}\left|\frac{\partial O_{\pi(n-1)}}{\partial f}\right|, \tag{19}$$

and define the error due the first $N$ largest contributions

$$\Delta\chi^2_N = \sum_{i=1}^{N}\left[\frac{1}{\sigma_{\pi(n)}}\frac{\partial O_{\pi(i)}}{\partial f}\right]^2 (\Delta f)^2_N \equiv 1 \tag{20}$$

so that the relative error is $\epsilon_N(f) = \Delta f_N/f$. We plot in Fig. 4 the result for $\epsilon_N(f^2) = 2\epsilon_N(f)$ and as we see about 10–20 data build the main contribution to the precision in $f^2$. These data correspond to the deuteron binding energy, the $np$ scattering length, low-energy $np$ total cross sections, and low-energy $pp$ differential cross sections.

TABLE VI. The $\chi^2$ results of the main combined $pp$ and $np$ partial-wave analysis for the 10 single-energy bins in the range $0 < T_{\rm LAB} < 350$ MeV.

| Bin (MeV) | $N_{pp}$ | $\chi^2_{pp}$ | $\chi^2_{pp}/N_{pp}$ | $N_{np}$ | $\chi^2_{np}$ | $\chi^2_{np}/N_{np}$ | $N$ | $\chi^2$ | $\chi^2/N$ |
|---|---|---|---|---|---|---|---|---|---|
| 0.0–0.5 | 103 | 107.2 | 1.04 | 46 | 88.2 | 1.92 | 149 | 195.4 | 1.31 |
| 0.5–2 | 82 | 58.8 | 0.72 | 50 | 92.8 | 1.86 | 132 | 151.5 | 1.15 |
| 2–8 | 92 | 80.1 | 0.87 | 122 | 151.0 | 1.24 | 214 | 231.0 | 1.08 |
| 8–17 | 124 | 100.3 | 0.81 | 229 | 183.9 | 0.80 | 353 | 284.1 | 0.80 |
| 17–35 | 111 | 85.5 | 0.77 | 346 | 324.2 | 0.94 | 457 | 409.7 | 0.90 |
| 35–75 | 261 | 231.2 | 0.89 | 513 | 559.7 | 1.09 | 774 | 790.9 | 1.02 |
| 75–125 | 152 | 154.8 | 1.02 | 399 | 445.2 | 1.12 | 551 | 600.0 | 1.09 |
| 125–183 | 301 | 300.5 | 1.00 | 372 | 381.7 | 1.03 | 673 | 682.2 | 1.01 |
| 183–290 | 882 | 905.0 | 1.03 | 858 | 841.4 | 0.98 | 1740 | 1746.4 | 1.00 |
| 290–350 | 898 | 956.1 | 1.06 | 798 | 808.1 | 1.01 | 1696 | 1764.1 | 1.04 |

TABLE VII. The pion-nucleon coupling constants $f_p^2$, $f_0^2$, and $f_c^2$ determined from different fits to the Granada-2013 database and their characteristics for the CD-OPE potential depending on the cutoff radius $r_c$. Charge dependence is only allowed on the $^1S_0$ partial wave.

| $r_c$(fm) | $f_p^2$ | $f_0^2$ | $f_c^2$ | $\chi^2_{pp}$ | $\chi^2_{np}$ | $\chi^2$ | $N_{\rm Dat}$ | $N_{\rm Par}$ | $\chi^2/\nu$ | $N_\sigma$ |
|---|---|---|---|---|---|---|---|---|---|---|
| 3.6 | 0.075 | | | 3065.13 | 3919.57 | 6984.71 | 6720 | 59 | 1.049 | 2.8 |
| 3.6 | 0.0697(3) | | | 3038.53 | 3913.10 | 6951.63 | 6720 | 60 | 1.044 | 2.5 |
| 3.6 | 0.0689(8) | 0.085(1) | 0.0703(8) | 3035.14 | 3897.41 | 6932.55 | 6720 | 62 | 1.041 | 2.4 |
| 3.0 | 0.075 | | | 2997.29 | 3957.57 | 6954.86 | 6720 | 46 | 1.042 | 2.4 |
| 3.0 | 0.0763(1) | | | 2995.20 | 3952.85 | 6947.05 | 6720 | 47 | 1.041 | 2.4 |
| 3.0 | 0.0764(4) | 0.0779(8) | 0.0758(4) | 2994.41 | 3950.42 | 6944.83 | 6720 | 49 | 1.041 | 2.4 |
| 2.4 | 0.75 | | | 3120.97 | 4028.61 | 7149.58 | 6718 | 39 | 1.070 | 4.1 |
| 2.4 | 0.07568(3) | | | 3116.56 | 4031.38 | 7147.94 | 6718 | 40 | 1.070 | 4.1 |
| 2.4 | 0.0768(3) | 0.0723(5) | 0.0750(3) | 3115.41 | 4017.76 | 7133.17 | 6718 | 42 | 1.068 | 4.0 |
| 1.8 | 0.75 | | | 4739.51 | 4230.16 | 8969.68 | 6709 | 31 | 1.343 | 19.8 |
| 1.8 | 0.076568(5) | | | 4725.30 | 4212.96 | 8938.26 | 6708 | 32 | 1.339 | 19.6 |
| 1.8 | 0.0763(2) | 0.0786(3) | 0.0765(2) | 4724.73 | 4198.16 | 8922.89 | 6708 | 34 | 1.337 | 19.5 |

TABLE VIII. The pion-nucleon coupling constant $f^2 = f_p^2 = f_0^2 = f_c^2$ and the chiral constants $c_1$, $c_3$, and $c_4$ determined from different fits to the Granada-2013 database and of the CD-OPE plus $\chi TPE$ depending on the cutoff radius $r_c$. Charge dependence is only allowed on the $^1S_0$ partial wave.

| $r_c$(fm) | $f^2$ | $c_1$ (GeV$^{-1}$) | $c_3$ (GeV$^{-1}$) | $c_4$ (GeV$^{-1}$) | $\chi^2_{pp}$ | $\chi^2_{np}$ | $\chi^2$ | $N_{\rm Dat}$ | $N_{\rm Par}$ | $\chi^2/\nu$ | $N_\sigma$ |
|---|---|---|---|---|---|---|---|---|---|---|---|
| 3.6 | 0.075 | 1010.0(306) | −990.9(264) | 9.6(140) | 2975.09 | 3879.15 | 6854.24 | 6719 | 63 | 1.030 | 1.7 |
| 3.6 | 0.0710(6) | 978.3(390) | −961.1(353) | −4.0(148) | 2965.28 | 3869.62 | 6834.90 | 6719 | 64 | 1.027 | 1.6 |
| 3.0 | 0.075 | −44.4(70) | 39.5(51) | −4.4(26) | 2979.46 | 3980.27 | 6959.73 | 6721 | 49 | 1.043 | 2.5 |
| 3.0 | 0.0763(3) | −35.2(79) | 31.3(60) | −6.4(27) | 2983.95 | 3968.28 | 6952.23 | 6721 | 50 | 1.042 | 2.4 |
| 2.4 | 0.075 | −10.6(18) | 5.2(10) | −2.1(8) | 3064.38 | 4049.88 | 7114.26 | 6718 | 41 | 1.065 | 3.8 |
| 2.4 | 0.0748(2) | −11.9(20) | 6.0(12) | −2.3(9) | 3065.80 | 4048.30 | 7114.11 | 6718 | 42 | 1.066 | 3.8 |
| 1.8 | 0.075 | −1.9(6) | −3.7(2) | 4.4(2) | 3101.24 | 4059.32 | 7160.56 | 6717 | 33 | 1.071 | 4.1 |
| 1.8 | 0.0763(2) | −1.6(6) | −3.7(3) | 4.3(2) | 3077.00 | 4050.22 | 7127.22 | 6717 | 34 | 1.066 | 3.8 |
| 1.2 | 0.075 | −11.17(9) | 0.76(2) | 2.822(2) | 3428.38 | 4659.52 | 8087.90 | 6715 | 25 | 1.209 | 12.1 |
| 1.2 | 0.07500(3) | −11.17(9) | 0.76(3) | 2.821(6) | 3428.28 | 4659.02 | 8087.31 | 6715 | 26 | 1.209 | 12.1 |

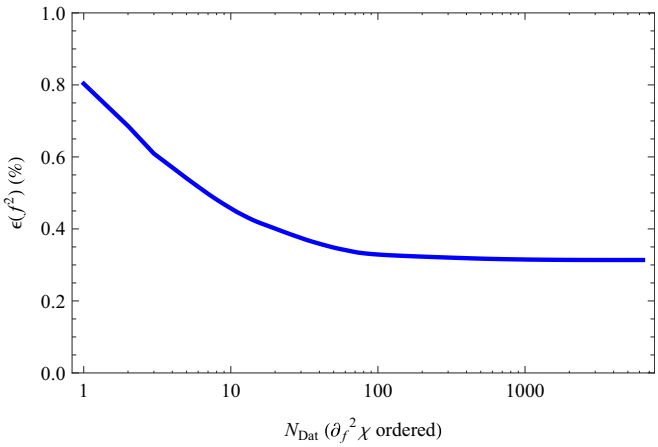


FIG. 4. Relative error in $f^2$ as a function of the number of data *ordered* according to a decreasing Hessian value.

### F. Systematics as a function of the number of data

As already mentioned, the Granada-2013 database is $3\sigma$ self-consistent according to our coarse-grained PWA. That implies that we can treat measurements as independent. On the other hand, we expect the precision will increase with the number of data. Of course, our selection of data is susceptible to change by gathering more data in the future. The Cramer-Rao inequality provides a lower bound on the error on the fitting parameters which can be determined from least-squares fitting [30]. Thus, errors will in general be *larger* than the $N_{\rm Dat} \to \infty$ case. Given the large amount of data considered in the present analysis, it is of utmost relevance to analyze this point in more detail.

Among the many ways of analyzing the systematic uncertainties, a particularly interesting one regards a chronological display of our self-consistent database as a function of the year where data where published and hence on the number of scattering data. This can be seen for $pp$ and $pp+np$ analysis separately in Tables IX and X, respectively, in 5-year intervals. As expected, accuracy improves when the total number of data $N_{\rm Dat}$ included in the analysis is increased. Most remarkable is the fact that, instead of the purely statistical estimate $\Delta f^2/f^2 \sim 1/\sqrt{N_{\rm Dat}}$, a fit to the actual trend reveals

TABLE IX. The pion-proton-proton coupling constant $f_p^2$ determined from different fits to the Granada-2013 database including only $pp$ data up to a given year.

| Year | $f_p^2$ | $\Delta f_p^2$ | $\chi^2_{pp}$ | $N_{pp}$ | $\chi^2_{pp}/N_{pp}$ |
|---|---|---|---|---|---|
| 1960 | 0.07867 | 0.00421 | 459.50 | 535 | 0.86 |
| 1965 | 0.07568 | 0.00210 | 669.05 | 748 | 0.89 |
| 1970 | 0.07273 | 0.00094 | 978.78 | 1137 | 0.86 |
| 1975 | 0.07317 | 0.00089 | 1149.63 | 1247 | 0.92 |
| 1980 | 0.07339 | 0.00069 | 1486.35 | 1585 | 0.94 |
| 1985 | 0.07443 | 0.00052 | 1559.43 | 1648 | 0.95 |
| 1990 | 0.07528 | 0.00050 | 1774.58 | 1831 | 0.97 |
| 1995 | 0.07542 | 0.00049 | 1809.02 | 1872 | 0.97 |
| 2000 | 0.07596 | 0.00043 | 2985.70 | 3003 | 0.99 |

TABLE X. The pion-nucleon-nucleon coupling constant $f^2$ determined from different fits to the Granada-2013 database including only data up to a given year.

| Year | $f^2$ | $\Delta f^2$ | $\chi^2_{pp}$ | $N_{pp}$ | $\chi^2_{np}$ | $N_{np}$ | $\chi^2/N$ |
|---|---|---|---|---|---|---|---|
| 1960 | 0.07860 | 0.00378 | 460.07 | 535 | 186.92 | 233 | 0.84 |
| 1965 | 0.07740 | 0.00192 | 671.34 | 748 | 791.65 | 836 | 0.92 |
| 1970 | 0.07427 | 0.00088 | 982.23 | 1137 | 922.94 | 981 | 0.90 |
| 1975 | 0.07504 | 0.00082 | 1156.39 | 1247 | 1145.81 | 1221 | 0.93 |
| 1980 | 0.07421 | 0.00061 | 1492.55 | 1585 | 2299.10 | 2311 | 0.97 |
| 1985 | 0.07499 | 0.00046 | 1580.77 | 1648 | 2612.23 | 2584 | 0.99 |
| 1990 | 0.07580 | 0.00043 | 1786.61 | 1831 | 2875.34 | 2806 | 1.01 |
| 1995 | 0.07607 | 0.00039 | 1821.38 | 1872 | 3022.34 | 2950 | 1.00 |
| 2000 | 0.07654 | 0.00034 | 2996.49 | 3003 | 3708.46 | 3528 | 1.03 |
| 2005 | 0.07631 | 0.00034 | 2995.27 | 3003 | 3827.69 | 3634 | 1.03 |
| 2013 | 0.07633 | 0.00014 | 2995.20 | 3003 | 3951.86 | 3717 | 1.03 |

more, $\Delta f^2/f^2 = 29.3/N_{\rm Dat}$, which is in fact better; see Fig. 5. This may be due to the fact that newer data tends to be more precise than older data. In fact, while the database contains more $np$ data than $pp$ data, the $pp$ data have smaller statistical errors and the corresponding fitting parameters tend to be better determined.

### G. Summary

The conclusion of all these investigations is that acceptable and natural fits produce smaller error bars than the purely statistical analysis presented in the previous section. This is probably due to the optimal sampling of the interaction complying with Nyquist theorem.

## VI. CONCLUSIONS

Since the strong proton-proton and neutron-neutron potentials correspond to the exchange of a neutral pion, the

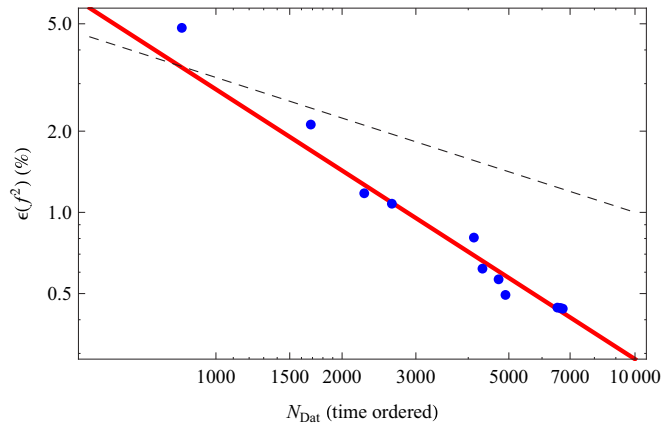


FIG. 5. Relative error in $f^2$ as a function of the number of data *ordered* according to their date of publication. Every point represents the number of $np+pp$ scattering data extracted from the Granada-2013 NN database and starting in 1960 forward in 5-year steps. We also show the statistical estimate $\epsilon(f^2) = 1/\sqrt{N_{\rm Par}}$ (black, dashed) and the fitting $\epsilon(f^2) = 30/N_{\rm Par}$ (red, solid).

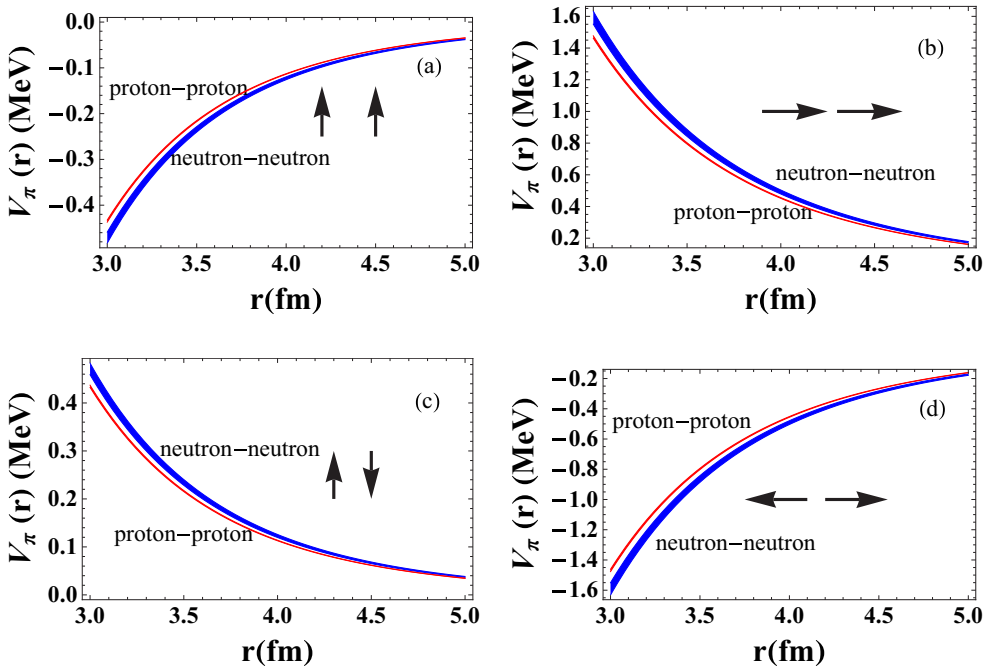


FIG. 6. Proton-proton and neutron-neutron interaction above 3 fm due to exchange of a neutral pion for different spin polarization states. The bands correspond to the statistical uncertainties from a fit to 6713 $np + pp$ scattering data below $T_{\rm LAB} = 350$ MeV with $\chi^2/\nu = 1.025$.

difference in the couplings manifests in the difference of the potentials above the estimated exclusive domain of the CD-OPE interaction. We can illustrate the main result pictorially in Fig. 6 by choosing the transversely and longitudinally polarized protons and neutrons. So we see that in any of the cases considered the strength of the $nn$ potential is stronger than the $pp$ potential, for instance, $|V_{n\uparrow,n\uparrow}| > |V_{p\uparrow,p\uparrow}|$ for $r > r_c = 3$ fm. Note that we cannot determine the neutron-neutron

TABLE XI. $pp$ isovector phase shifts.

| $E_{\rm LAB}$ | $^1S_0$ | $^1D_2$ | $^1G_4$ | $^3P_0$ | $^3P_1$ | $^3F_3$ | $^3P_2$ | $\epsilon_2$ | $^3F_2$ | $^3F_4$ | $\epsilon_4$ | $^3H_4$ |
|---|---|---|---|---|---|---|---|---|---|---|---|---|
| 1 | 32.674 | 0.001 | 0.000 | 0.135 | − 0.081 | − 0.000 | 0.014 | − 0.001 | 0.000 | 0.000 | − 0.000 | 0.000 |
| | ± 0.003 | | | | | | | | | | | |
| 5 | 54.836 | 0.043 | 0.000 | 1.599 | − 0.901 | − 0.004 | 0.213 | − 0.052 | 0.002 | 0.000 | − 0.000 | 0.000 |
| | ± 0.008 | | | ± 0.005 | ± 0.003 | | ± 0.001 | | | | | |
| 10 | 55.238 | 0.166 | 0.003 | 3.772 | − 2.054 | − 0.032 | 0.648 | − 0.204 | 0.013 | 0.001 | − 0.004 | 0.000 |
| | ± 0.011 | ± 0.001 | | ± 0.011 | ± 0.006 | | ± 0.002 | ± 0.001 | | | | |
| 25 | 48.759 | 0.699 | 0.040 | 8.666 | − 4.888 | − 0.234 | 2.490 | − 0.820 | 0.107 | 0.019 | − 0.050 | 0.004 |
| | ± 0.014 | ± 0.002 | | ± 0.027 | ± 0.010 | ± 0.001 | ± 0.006 | ± 0.003 | ± 0.001 | | | |
| 50 | 39.133 | 1.711 | 0.154 | 11.577 | − 8.224 | − 0.696 | 5.856 | − 1.719 | 0.346 | 0.104 | − 0.200 | 0.027 |
| | ± 0.018 | ± 0.004 | ± 0.001 | ± 0.046 | ± 0.013 | ± 0.004 | ± 0.011 | ± 0.005 | ± 0.002 | ± 0.001 | ± 0.001 | |
| 100 | 25.340 | 3.774 | 0.422 | 9.535 | − 13.260 | − 1.502 | 10.986 | − 2.650 | 0.842 | 0.466 | − 0.561 | 0.112 |
| | ± 0.036 | ± 0.009 | ± 0.002 | ± 0.072 | ± 0.021 | ± 0.010 | ± 0.024 | ± 0.009 | ± 0.009 | ± 0.005 | ± 0.002 | ± 0.001 |
| 150 | 15.116 | 5.618 | 0.703 | 4.839 | − 17.637 | − 2.077 | 14.021 | − 2.921 | 1.203 | 1.019 | − 0.883 | 0.225 |
| | ± 0.050 | ± 0.015 | ± 0.006 | ± 0.079 | ± 0.027 | ± 0.020 | ± 0.023 | ± 0.013 | ± 0.017 | ± 0.010 | ± 0.003 | ± 0.002 |
| 200 | 6.892 | 7.206 | 1.000 | − 0.214 | − 21.554 | − 2.471 | 15.803 | − 2.907 | 1.334 | 1.638 | − 1.133 | 0.351 |
| | ± 0.060 | ± 0.022 | ± 0.012 | ± 0.071 | ± 0.039 | ± 0.037 | ± 0.027 | ± 0.017 | ± 0.023 | ± 0.017 | ± 0.005 | ± 0.006 |
| 250 | 0.178 | 8.552 | 1.295 | − 5.098 | − 24.984 | − 2.623 | 16.739 | − 2.698 | 1.224 | 2.205 | − 1.311 | 0.479 |
| | ± 0.075 | ± 0.025 | ± 0.017 | ± 0.068 | ± 0.055 | ± 0.054 | ± 0.034 | ± 0.023 | ± 0.029 | ± 0.024 | ± 0.006 | ± 0.013 |
| 300 | − 5.222 | 9.571 | 1.571 | − 9.601 | − 27.919 | − 2.418 | 16.981 | − 2.293 | 0.918 | 2.659 | − 1.439 | 0.591 |
| | ± 0.102 | ± 0.032 | ± 0.019 | ± 0.095 | ± 0.070 | ± 0.066 | ± 0.034 | ± 0.032 | ± 0.041 | ± 0.029 | ± 0.008 | ± 0.020 |
| 350 | − 9.447 | 10.140 | 1.832 | − 13.545 | − 30.348 | − 1.820 | 16.635 | − 1.707 | 0.454 | 3.012 | − 1.552 | 0.670 |
| | ± 0.138 | ± 0.055 | ± 0.027 | ± 0.152 | ± 0.082 | ± 0.080 | ± 0.031 | ± 0.042 | ± 0.058 | ± 0.047 | ± 0.010 | ± 0.027 |

TABLE XII. *np* isovector phase shifts.

| $E_{\rm LAB}$ | $^1S_0$ | $^1D_2$ | $^1G_4$ | $^3P_0$ | $^3P_1$ | $^3F_3$ | $^3P_2$ | $\epsilon_2$ | $^3F_2$ | $^3F_4$ | $\epsilon_4$ | $^3H_4$ |
|---|---|---|---|---|---|---|---|---|---|---|---|---|
| 1 | 62.047 | 0.001 | 0.000 | 0.183 | −0.105 | −0.000 | 0.025 | −0.001 | 0.000 | 0.000 | −0.000 | 0.000 |
| | ± 0.024 | | | ± 0.003 | ± 0.002 | | | | | | | |
| 5 | 63.559 | 0.041 | 0.000 | 1.683 | −0.911 | −0.004 | 0.284 | −0.049 | 0.002 | 0.000 | −0.000 | 0.000 |
| | ± 0.046 | ± 0.001 | | ± 0.029 | ± 0.016 | | ± 0.004 | ± 0.001 | | | | |
| 10 | 59.851 | 0.155 | 0.002 | 3.823 | −1.996 | −0.026 | 0.796 | −0.185 | 0.011 | 0.001 | −0.003 | 0.000 |
| | ± 0.053 | ± 0.003 | | ± 0.058 | ± 0.031 | ± 0.001 | ± 0.009 | ± 0.004 | | | | |
| 25 | 50.712 | 0.673 | 0.032 | 8.699 | −4.666 | −0.195 | 2.846 | −0.765 | 0.091 | 0.017 | −0.040 | 0.003 |
| | ± 0.062 | ± 0.012 | ± 0.001 | ± 0.096 | ± 0.053 | ± 0.005 | ± 0.027 | ± 0.014 | ± 0.002 | ± 0.001 | ± 0.001 | |
| 50 | 40.225 | 1.695 | 0.134 | 11.682 | −7.822 | −0.594 | 6.364 | −1.660 | 0.309 | 0.105 | −0.170 | 0.021 |
| | ± 0.083 | ± 0.019 | ± 0.003 | ± 0.109 | ± 0.059 | ± 0.015 | ± 0.045 | ± 0.020 | ± 0.006 | ± 0.004 | ± 0.004 | ± 0.001 |
| 100 | 26.129 | 3.760 | 0.391 | 9.484 | −12.592 | −1.299 | 11.070 | −2.658 | 0.780 | 0.514 | −0.507 | 0.095 |
| | ± 0.138 | ± 0.018 | ± 0.009 | ± 0.163 | ± 0.080 | ± 0.036 | ± 0.061 | ± 0.009 | ± 0.013 | ± 0.021 | ± 0.011 | ± 0.002 |
| 150 | 15.917 | 5.568 | 0.671 | 4.399 | −16.716 | −1.915 | 13.334 | −3.000 | 1.117 | 1.130 | −0.828 | 0.204 |
| | ± 0.191 | ± 0.017 | ± 0.013 | ± 0.216 | ± 0.120 | ± 0.062 | ± 0.082 | ± 0.020 | ± 0.020 | ± 0.039 | ± 0.015 | ± 0.005 |
| 200 | 7.810 | 7.118 | 0.961 | −1.038 | −20.374 | −2.536 | 14.510 | −3.028 | 1.217 | 1.773 | −1.091 | 0.334 |
| | ± 0.243 | ± 0.023 | ± 0.017 | ± 0.261 | ± 0.170 | ± 0.085 | ± 0.109 | ± 0.027 | ± 0.024 | ± 0.054 | ± 0.014 | ± 0.011 |
| 250 | 1.289 | 8.435 | 1.238 | −6.196 | −23.543 | −2.989 | 15.158 | −2.834 | 1.072 | 2.318 | −1.290 | 0.464 |
| | ± 0.302 | ± 0.025 | ± 0.020 | ± 0.304 | ± 0.224 | ± 0.101 | ± 0.125 | ± 0.030 | ± 0.030 | ± 0.070 | ± 0.010 | ± 0.018 |
| 300 | −3.856 | 9.421 | 1.488 | −10.830 | −26.215 | −2.958 | 15.386 | −2.426 | 0.733 | 2.732 | −1.441 | 0.561 |
| | ± 0.367 | ± 0.033 | ± 0.021 | ± 0.356 | ± 0.274 | ± 0.135 | ± 0.122 | ± 0.036 | ± 0.042 | ± 0.090 | ± 0.008 | ± 0.027 |
| 350 | −7.791 | 9.947 | 1.720 | −14.770 | −28.375 | −2.224 | 15.185 | −1.828 | 0.244 | 3.053 | −1.574 | 0.593 |
| | ± 0.439 | ± 0.057 | ± 0.028 | ± 0.427 | ± 0.318 | ± 0.250 | ± 0.107 | ± 0.045 | ± 0.059 | ± 0.126 | ± 0.011 | ± 0.036 |

interaction below $r_c$, and in particular the corresponding neutron-neutron scattering length cannot be determined from the present calculation.

We summarize our points. Using the $3\sigma$ self-consistent Granada-2013 database for *np* and *pp* scattering comprising LAB energies below 350 MeV, we have investigated isospin breaking in the pion-nucleon coupling constants by separating the nuclear potential in two distinct contributions: Above 3 fm, we use charge-dependent one-pion exchange potential for the strong part along with electromagnetic and relativistic

TABLE XIII. *np* isoscalar phase shifts.

| $E_{\rm LAB}$ | $^1P_1$ | $^1F_3$ | $^3D_2$ | $^3G_4$ | $^3S_1$ | $\epsilon_1$ | $^3D_1$ | $^3D_3$ | $\epsilon_3$ | $^3G_3$ |
|---|---|---|---|---|---|---|---|---|---|---|
| 1 | −0.191 | −0.000 | 0.006 | 0.000 | 147.685 | 0.105 | −0.005 | 0.000 | 0.000 | −0.000 |
| | | | | | ± 0.017 | ± 0.001 | | | | |
| 5 | −1.528 | −0.010 | 0.226 | 0.001 | 118.043 | 0.654 | −0.186 | 0.002 | 0.013 | −0.000 |
| | ± 0.003 | | | | ± 0.024 | ± 0.005 | | | | |
| 10 | −3.119 | −0.066 | 0.876 | 0.012 | 102.425 | 1.112 | −0.690 | 0.005 | 0.083 | −0.003 |
| | ± 0.009 | | ± 0.001 | | ± 0.034 | ± 0.011 | ± 0.002 | | | |
| 25 | −6.413 | −0.435 | 3.839 | 0.177 | 80.364 | 1.696 | −2.843 | 0.039 | 0.572 | −0.055 |
| | ± 0.029 | | ± 0.010 | | ± 0.059 | ± 0.026 | ± 0.009 | ± 0.001 | | |
| 50 | −9.656 | −1.173 | 9.265 | 0.755 | 62.489 | 2.032 | −6.496 | 0.292 | 1.658 | −0.274 |
| | ± 0.062 | ± 0.002 | ± 0.037 | ± 0.001 | ± 0.078 | ± 0.047 | ± 0.026 | ± 0.005 | ± 0.004 | ± 0.001 |
| 100 | −14.214 | −2.304 | 17.776 | 2.321 | 43.135 | 2.515 | −12.295 | 1.321 | 3.532 | −1.007 |
| | ± 0.097 | ± 0.015 | ± 0.076 | ± 0.014 | ± 0.086 | ± 0.082 | ± 0.054 | ± 0.020 | ± 0.018 | ± 0.011 |
| 150 | −18.203 | −3.097 | 22.620 | 3.986 | 30.862 | 2.927 | −16.683 | 2.338 | 4.833 | −1.873 |
| | ± 0.114 | ± 0.036 | ± 0.096 | ± 0.045 | ± 0.098 | ± 0.110 | ± 0.081 | ± 0.042 | ± 0.031 | ± 0.036 |
| 200 | −21.765 | −3.831 | 24.866 | 5.583 | 21.462 | 3.272 | −20.284 | 2.931 | 5.790 | −2.718 |
| | ± 0.142 | ± 0.053 | ± 0.123 | ± 0.080 | ± 0.123 | ± 0.131 | ± 0.114 | ± 0.067 | ± 0.040 | ± 0.064 |
| 250 | −24.856 | −4.634 | 25.699 | 7.011 | 13.557 | 3.677 | −23.290 | 3.067 | 6.565 | −3.516 |
| | ± 0.181 | ± 0.061 | ± 0.149 | ± 0.102 | ± 0.148 | ± 0.142 | ± 0.130 | ± 0.095 | ± 0.055 | ± 0.083 |
| 300 | −27.487 | −5.498 | 25.991 | 8.197 | 6.566 | 4.262 | −25.639 | 2.870 | 7.195 | −4.314 |
| | ± 0.221 | ± 0.077 | ± 0.194 | ± 0.117 | ± 0.171 | ± 0.175 | ± 0.143 | ± 0.129 | ± 0.069 | ± 0.101 |
| 350 | −29.666 | −6.335 | 26.295 | 9.101 | 0.223 | 5.068 | −27.156 | 2.492 | 7.647 | −5.173 |
| | ± 0.257 | ± 0.129 | ± 0.312 | ± 0.142 | ± 0.193 | ± 0.265 | ± 0.210 | ± 0.166 | ± 0.082 | ± 0.146 |

corrections. Below 3 fm, we regard the interaction as unknown and we coarse grain it down to the shortest de Broglie wavelength corresponding to the pion production threshold, which is about 0.6 fm. With a total number of 55 parameters, including the three pion-nucleon coupling constants, we describe a total number of 6741 $np$ and $pp$ data including normalization factors provided by the experimentalist which a total $\chi^2$ of 6855.5, which means $\chi^2/\nu = 1.025$. We see clear evidence that the coupling of neutral pions to neutrons is larger than to protons. As a consequence, neutrons interact more strongly than protons.

## ACKNOWLEDGMENTS

We thank C. Dominguez, J. Ruiz de Elvira, and J. L. Goity for discussions. This work was supported by Spanish Ministerio de Economia y Competitividad and European FEDER funds (Grant No. FIS2014-59386-P) and by the Agencia de Innovacion y Desarrollo de Andalucia (Grant No. FQM225). This work was partly performed under the auspices of the U.S. Department of Energy by Lawrence Livermore National Laboratory under Contract No. DE-AC52-07NA27344. Funding was also provided by the U.S. Department of Energy, Office of Science, Office of Nuclear Physics under Award No. DE-SC0008511 (NUCLEI SciDAC Collaboration)

## APPENDIX A: OPERATOR BASIS

To incorporate charge dependence on $P$ waves, two more operators need to be added to the basis we used previously, getting a total of 23 operators $O^n$. The potential is written as a sum of functions multiplied by each operator

$$V(r) = \sum_{n=1,23} V_n(r) O^n. \tag{A1}$$

The first fourteen operators are charge independent and correspond to the ones used in the Argonne $v_{14}$ potential

$$O^{n=1,14} = 1, \boldsymbol{\tau}_1\cdot\boldsymbol{\tau}_2, \boldsymbol{\sigma}_1\cdot\boldsymbol{\sigma}_2, (\boldsymbol{\sigma}_1\cdot\boldsymbol{\sigma}_2)(\boldsymbol{\tau}_1\cdot\boldsymbol{\tau}_2), S_{12}, S_{12}(\boldsymbol{\tau}_1\cdot\boldsymbol{\tau}_2), \mathbf{L}\cdot\mathbf{S}, \mathbf{L}\cdot\mathbf{S}(\boldsymbol{\tau}_1\cdot\boldsymbol{\tau}_2), L^2, L^2(\boldsymbol{\tau}_1\cdot\boldsymbol{\tau}_2), L^2(\boldsymbol{\sigma}_1\cdot\boldsymbol{\sigma}_2), L^2(\boldsymbol{\sigma}_1\cdot\boldsymbol{\sigma}_2)(\boldsymbol{\tau}_1\cdot\boldsymbol{\tau}_2), (\mathbf{L}\cdot\mathbf{S})^2, (\mathbf{L}\cdot\mathbf{S})^2(\boldsymbol{\tau}_1\cdot\boldsymbol{\tau}_2). \tag{A2}$$

These fourteen components are denoted by $c$, $\tau$, $\sigma$, $\sigma\tau$, $t$, $t\tau$, $ls$, $ls\tau$, $l2$, $l2\tau$, $l2\sigma$, $l2\sigma\tau$, $ls2$, and $ls2\tau$. The remaining charge-dependent operators are

$$O^{n=15,21} = T_{12}, (\boldsymbol{\sigma}_1\cdot\boldsymbol{\sigma}_2)T_{12}, S_{12}T_{12}, (\tau_{z1}+\tau_{z2}), (\boldsymbol{\sigma}_1\cdot\boldsymbol{\sigma}_2)(\tau_{z1}+\tau_{z2}), L^2T_{12}, L^2(\boldsymbol{\sigma}_1\cdot\boldsymbol{\sigma}_2)T_{12}, \mathbf{L}\cdot\mathbf{S}T_{12}, (\mathbf{L}\cdot\mathbf{S})^2T_{12}, \tag{A3}$$

and are labeled as $T$, $\sigma T$, $tT$, $\tau z$, $\sigma\tau z$, $l2T$, $l2\sigma T$, $lsT$, and $ls2T$. The first five were introduced by Wiringa *et al.* in Ref. [62]; the following two were included in Ref. [34] to restrict the charge dependence to the $^1S_0$ by following certain linear dependence relations between $V_T$, $V_{\sigma T}$, $V_{l2T}$, and $V_{l2\sigma T}$. The last two terms are required for the charge dependence on the $^3P_0$, $^3P_1$, and $^3P_2$ partial waves.

As in our previous analysis, we set $V_{tT} = V_{\tau z} = V_{\sigma\tau z} = 0$ to exclude charge dependence on the tensor terms and charge asymmetries. To restrict the charge dependence to the $S$ and $P$ waves parameters, the remaining potential functions must follow

$$48V_{l2T} = -5V_T + 3V_{\sigma T} + 12V_{lsT} - 48V_{ls2T}, \tag{A4}$$

$$48V_{\sigma l2T} = V_T - 7V_{\sigma T} + 4V_{lsT} - 16V_{ls2T}. \tag{A5}$$

## APPENDIX B: PHASE SHIFTS

In Tables XI, XII, and XIII we provide the $pp$ and $np$ phase shifts for the lower partial waves and selected LAB energies with their corresponding error bars for the fit with charge dependence in $S$ and $P$ waves. In the case that errors are smaller than $10^{-3}$, we leave the cell empty.

[1] H. Yukawa, Proc. Phys. Math. Soc. Jpn. **17**, 48 (1935).
[2] W. Pauli, *Meson Theory of Nuclear Forces* (Interscience Publishers, New York, 1948).
[3] O. Dumbrajs *et al.*, Nucl. Phys. B **216**, 277 (1983).
[4] J. de Swart, M. Rentmeester, and R. Timmermans, PiN Newslett. **13**, 96 (1997).
[5] M. Sainio, PiN Newslett. **15**, 156 (1999).
[6] D. Bugg, Eur. Phys. J. C **33**, 505 (2004).
[7] H. A. Bethe, Phys. Rev. **57**, 260 (1940).
[8] H. Bethe, Phys. Rev. **57**, 390 (1940).
[9] M. L. Goldberger and S. B. Treiman, Phys. Rev. **110**, 1178 (1958).
[10] Y. Nambu, Phys. Rev. Lett. **4**, 380 (1960).
[11] G. F. Chew, Phys. Rev. **112**, 1380 (1958).
[12] P. Cziffra *et al.*, Phys. Rev. **114**, 880 (1959).
[13] M. H. MacGregor, M. J. Moravcsik, and H. P. Stapp, Phys. Rev. **116**, 1248 (1959).
[14] P. S. Signell, Phys. Rev. Lett. **5**, 474 (1960).
[15] M. MacGregor, R. Arndt, and A. Dubow, Phys. Rev. **135**, B628 (1964).
[16] D. V. Bugg, A. A. Carter, and J. R. Carter, Phys. Lett. B **44**, 278 (1973).
[17] R. A. Arndt, Z. Li, L. D. Roper, and R. L. Workman, Phys. Rev. Lett. **65**, 157 (1990).
[18] R. A. Arndt, R. L. Workman, and M. M. Pavan, Phys. Rev. C **49**, 2729 (1994).
[19] T. E. O. Ericson, B. Loiseau, and A. W. Thomas, Phys. Rev. C **66**, 014005 (2002).
[20] R. A. Arndt, W. J. Briscoe, I. I. Strakovsky, and R. L. Workman, Phys. Rev. C **74**, 045205 (2006).
[21] V. Baru *et al.*, Phys. Lett. B **694**, 473 (2011).
[22] V. Baru *et al.*, Nucl. Phys. A **872**, 69 (2011).
[23] R. G. E. Timmermans, T. A. Rijken, and J. J. de Swart, Phys. Rev. Lett. **67**, 1074 (1991).
[24] V. G. J. Stoks, R. A. M. Klomp, M. C. M. Rentmeester, and J. J. deSwart, Phys. Rev. C **48**, 792 (1993).

[25] R. A. M. Klomp, V. G. J. Stoks, and J. J. de Swart, Phys. Rev. C **44**, R1258(R) (1991).
[26] V. Stoks, R. Timmermans, and J. J. de Swart, Phys. Rev. C **47**, 512 (1993).
[27] N. Kaiser, R. Brockmann, and W. Weise, Nucl. Phys. A **625**, 758 (1997).
[28] M. C. M. Rentmeester, R. G. E. Timmermans, J. L. Friar, and J. J. de Swart, Phys. Rev. Lett. **82**, 4992 (1999).
[29] M. C. M. Rentmeester, R. G. E. Timmermans, and J. J. de Swart, Phys. Rev. C **67**, 044001 (2003).
[30] M. J. Evans and J. S. Rosenthal, *Probability and Statistics: The Science of Uncertainty* (Macmillan, New York, 2004).
[31] J. Dobaczewski, W. Nazarewicz, and P. G. Reinhard, J. Phys. G **41**, 074001 (2014).
[32] J. R. Bergervoet, P. C. van Campen, W. A. van der Sanden, and J. J. de Swart, Phys. Rev. C **38**, 15 (1988).
[33] R. Navarro Pérez, J. E. Amaro, and E. Ruiz Arriola, Few Body Syst. **55**, 983 (2014).
[34] R. Navarro Pérez, J. E. Amaro, and E. Ruiz Arriola, Phys. Rev. C **88**, 064002 (2013); **91**, 029901(E) (2015).
[35] R. Navarro Pérez, J. E. Amaro, and E. Ruiz Arriola, Phys. Rev. C **89**, 064006 (2014).
[36] R. Navarro Pérez, J. E. Amaro, and E. Ruiz Arriola, J. Phys. G **42**, 034013 (2015).
[37] The 2013 Granada database is available at http://www.ugr.es/amaro/nndatabase/
[38] S. Aldor-Noiman *et al.*, Am. Statist. **67**, 249 (2013).
[39] R. Navarro Pérez, E. Ruiz Arriola, and J. R. de Elvira, Phys. Rev. D **91**, 074014 (2015).
[40] T. E. O. Ericson, B. Loiseau, J. Nilsson, N. Olsson, J. Blomgren, H. Condé, K. Elmgren, O. Jonsson, L. Nilsson, P.-U. Renberg, A. Ringbom *et al.*, Phys. Rev. Lett. **75**, 1046 (1995).
[41] J. Rahm, J. Blomgren, H. Condé, S. Dangtip, K. Elmgren, N. Olsson, T. Rönnqvist, R. Zorro, A. Ringbom, G. Tibell *et al.*, Phys. Rev. C **57**, 1077 (1998).
[42] S. Weinberg, *The Quantum Theory of Fields* (Cambridge University Press, Cambridge, UK, 2013), Vol. 2.
[43] M. C. M. Rentmeester, R. A. M. Klomp, and J. J. de Swart, Phys. Rev. Lett. **81**, 5253 (1998).
[44] T. E. O. Ericson, B. Loiseau, J. Rahm, N. Olsson, J. Blomgren, H. Condé, K. Elmgren, O. Jonsson, L. Nilsson, P.-U. Renberg *et al.*, Phys. Rev. Lett. **81**, 5254 (1998).
[45] J. Blomgren (ed.), Phys. Scr. T **87**, 1 (2000).
[46] M. Sarsour, T. Peterson, M. Planinic, S. E. Vigdor, C. Allgower, B. Bergenwall, J. Blomgren, T. Hossbach, W. W. Jacobs, C. Johansson *et al.*, Phys. Rev. Lett. **94**, 082303 (2005).
[47] M. Sarsour, T. Peterson, M. Planinic, S. E. Vigdor, C. Allgower, B. Bergenwall, J. Blomgren, T. Hossbach, W. W. Jacobs, C. Johansson *et al.*, Phys. Rev. C **74**, 044003 (2006).
[48] HAL QCD Collaboration, S. Aoki, Prog. Part. Nucl. Phys. **66**, 687 (2011).
[49] S. Aoki, Eur. Phys. J. A **49**, 81 (2013).
[50] S. Aoki, T. Hatsuda, and N. Ishii, Prog. Theor. Phys. **123**, 89 (2010).
[51] J. B. Aviles, Phys. Rev. C **6**, 1467 (1972).
[52] R. Navarro Pérez, J. E. Amaro, and E. Ruiz Arriola, Int. J. Mod. Phys. E **25**, 1641009 (2016).
[53] C. A. Dominguez, Riv. Nuovo Cimento **8**, 1 (1985).
[54] J. L. Goity *et al.*, Phys. Lett. B **454**, 115 (1999).
[55] J. Goity and J. Saez, Report JLAB-THY-03-26, Jefferson Laboratory, Newport News (Virgina), 2002.
[56] V. Bernard, N. Kaiser, and U. G. Meissner, Nucl. Phys. A **615**, 483 (1997).
[57] T. Ledwig, J. Nieves, A. Pich, E. Ruiz Arriola, and J. R. de Elvira, Phys. Rev. D **90**, 114020 (2014).
[58] A. W. Thomas and K. Holinde, Phys. Rev. Lett. **63**, 2025 (1989).
[59] R. Braun *et al.*, Phys. Lett. B **660**, 161 (2008).
[60] F. Gross and A. Stadler, Phys. Lett. B **668**, 163 (2008).
[61] G. J. Weisel, R. T. Braun, and W. Tornow, Phys. Rev. C **82**, 027001 (2010).
[62] R. B. Wiringa, V. G. J. Stoks, and R. Schiavilla, Phys. Rev. C **51**, 38 (1995).
[63] R. Machleidt, Phys. Rev. C **63**, 024001 (2001).
[64] R. Navarro Pérez, J. E. Amaro, and E. Ruiz Arriola, Phys. Rev. C **89**, 024004 (2014).
[65] R. Navarro Pérez, J. E. Amaro, and E. Ruiz Arriola, Phys. Rev. C **88**, 024002 (2013); **88**, 069902(E) (2013).
[66] V. Stoks and J. J. de Swart, Phys. Rev. C **47**, 761 (1993).
[67] V. G. J. Stoks and J. J. de Swart, Phys. Rev. C **52**, 1698 (1995).
[68] N. Hoshizaki, Prog. Theor. Phys. Suppl. **42**, 107 (1968).
[69] J. Bystricky, F. Lehar, and P. Winternitz, J. Phys. (France) **39**, 1 (1978).
[70] E. Ruiz Arriola, J. E. Amaro, and R. Navarro Pérez, Mod. Phys. Lett. A **31**, 1630027 (2016).
[71] R. Navarro Pérez, J. E. Amaro, and E. Ruiz Arriola, Phys. Rev. C **91**, 054002 (2015).
[72] E. Ruiz Arriola, J. E. Amaro, and R. Navarro Pérez, EPJ Web Conf. **137**, 09006 (2017).
[73] R. Navarro Pérez, J. E. Amaro, and E. Ruiz Arriola, J. Phys. G **43**, 114001 (2016).
[74] I. R. Simo, R. Navarro Pérez, J. E. Amaro, and E. Ruiz Arriola, Phys. Rev. C **95**, 054003 (2017).
[75] R. Navarro Pérez, J. E. Amaro, and E. Ruiz Arriola, PoS C **D12**, 104 (2013).
[76] D. Siemens *et al.*, Phys. Lett. B **770**, 27, 2017.